A new method to correlate Thermal Mathematical Models of space instruments and payloads

Ignacio Torralbo[⋆†]*, Javier Piqueras*[⋆]*, Isabel Pérez-Grande*[⋆] *and Angel Sanz-Andrés*[⋆]
[⋆]*IDR/ETSIAE Universidad Politécnica de Madrid*
Address
ignacio.torralbo@upm.es · javier.piqueras@upm.es · isabel.perez.grande@upm.es · angel.sanz.andres@upm.es
[†]Corresponding author

Abstract

The correlation of the Thermal Mathematical Models is often performed manually, and the results obtained in this way are generally not the optimum and could be improved with other strategies. A method of correlation is presented for for steady-state cases. The method is based on a Jacobian matrix formulation and a Moore-Penrose pseudo-inversion. The formulation allows the correlation of a model with several load cases, as it is the usual case in space projects. As an example, it has been applied to the thermal mathematical model of the Optics Unit of the instrument PHI of the ESA Solar Orbiter mission.

1. Introduction

The thermal mathematical model (TMM) plays a very important role during all the phases of a space mission. The numbers of nodes in the models normally increases as the design grows. For these reason, at some point, a Reduced Thermal Mathematical Model (RTMM) is developed. The RTMM is derived from the Detailed Mathematical Model (DTMM) with the aim of reproducing the same results but with much fewer number of nodes. For these reason, the two models have to be correlated.

Quite often, the correlation process is performed manually. If this the case, good engineering skills and expertise is needed. However, to facilitate the process, the use of mathematical tools can be of great help[1,5,6,10] . The goal of these tools is to reduce the correlation time and minimize the error of the model results with regard to the reference data. Therefore, the correlation process can be considered as an optimization problem. In most cases, the thermal mathematical model to be correlated has been built with an estimation of value of the parameters, based on good engineering knowledge. This means that the value of the parameters to be adjusted during the correlation are not really far from the optimum solution. If the iteration is started with these estimated initial values, the thermal mathematical models usually show a smooth and monotonous dependence on the parameters around these values. The method here proposed is based on the manipulation of the Jacobian matrix. The advantage with respect to previous methods is that many load cases can be correlated simultaneously.

The process of correlation is same for the correlation of the thermal mathematical model with respect to reference data from tests or from other TMM. The TMM must be correlated for different load cases. Each load case is represented by a set of boundary conditions, defining the different scenarios of the mission. To have reliable predictions the TMM must be correlated in the different scenarios. In the correlation process each scenario is defined by a set of reference temperatures.

In the thermal control of space instruments is a common practice to study two extreme cases. The first one is given by the hottest conditions and the second by the coldest. Given this two cases, the temperatures of the entire mission are assumed to be somewhere inside these limits. If a TMM is only correlated with one set of reference temperatures, probably the prediction outside this conditions wont be acceptable.

The correlation method presented has been proven in the Polarimetric Helioseismic Imager Optics Unit of Solar Orbiter mission,[3] PHI O-Unit. In order to test the method in a small-size model, the reduced thermal mathematical model of the unit has been correlated with the detailed mathematical model. For this correlation two different load cases have been used, the cold operational and the hot operational cases, and the results presented.

2. Correlation method

The method proposed[13] consists in the use of a generalized Jacobian matrix and Moore-Penrose pseudo inverse to solve the model to reference data correlation problem by least square minimization of the error.

The correlation process can be considered a optimization problem as we want to minimize the sum squared deviations E_T as,

$$E_T(X) = \sum_{j=1}^{N_N} \left(T_{R_j} - T_j(X)\right)^2 \tag{1}$$

where N_N is the number of nodes in the TMM, T_R is the reference temperature and $T_j(X)$ is the estimated temperature of the TMM with the parameters X. As we want to find the minimum error we can evaluate the gradient of the (1) and the condition of minimum will occur when $\nabla_X E_T = 0$,

$$\frac{\partial E_T}{\partial X_i} = \sum_{j=1}^{N_N} \frac{\partial E_T}{\partial T_j} \frac{\partial T_j}{\partial X_i} = -2 \sum_{j=1}^{N_N} \left(T_{Rj} - T_j(X)\right) \frac{\partial T_j(X)}{\partial X_i} = 0, \qquad i = 1...N_P \tag{2}$$

where $\frac{\partial T_j(X)}{\partial X_i}$ corresponds with the terms of the Jacobian matrix, $\mathbf{M}$. and N_P is the number of parameters.

$$M_{ji} = \frac{\partial T_j(X)}{\partial X_i} \tag{3}$$

If we assume a monotonous dependence of T on X, a local linear dependence can be defined between both set of coordinates (Using Taylor Series expansion[11]),

$$T = T^0 + \sum_{h}^{N_p} \frac{\partial t}{\partial x_h} x_h \tag{4}$$

where T^0 is the estimated temperatures with the initial guess of the parameters. Using this expression and writing the fluctuations around the initial point as $t_{R_j} = T_{R_j} - T_j^0$ and $x_{R_j} = X_{R_j} - X_j^0$, the expression (2) can be expressed as,

$$\mathbf{M}^T t_R - \left(x^T \mathbf{M}^T \mathbf{M}\right)^T = 0 \tag{5}$$

where we have used the jacobian matrix (3). This N_P equation system can be solved for x by left multiplying it by the inverse of $\mathbf{M_C} = \mathbf{M^T M}$, if it is non-singular. $\mathbf{M_C}$ is a square symmetric matrix, N_P x N_P size. Therefore, the solution[11] x is,

$$x^* = \mathbf{M}^+ t_R \qquad \text{where} \qquad \mathbf{M}^+ = \left(\mathbf{M}^T \mathbf{M}\right)^{-1} \mathbf{M}^T \tag{6}$$

This solution can be generalised for several load cases following the same procedure. If we define the error, (1) for two different load cases,

$$\sum_{j=1}^{N_N} \left(T_{R_j} - T_j\right) \frac{\partial t_j}{\partial x_i}\bigg|_{C_1} + \sum_{j=1}^{N_N} \left(T_{R_j} - T_j\right) \frac{\partial t_j}{\partial x_i}\bigg|_{C_2} = 0 \tag{7}$$

where C_1 and C_2 are the two load cases. Using the same argumentation as in (4) and (3),

$$\mathbf{M}^T t_R\big|_{C_1} + \mathbf{M}^T t_R\big|_{C_2} = \left(\mathbf{M}^T \mathbf{M}\big|_{C_1} + \mathbf{M}^T \mathbf{M}\big|_{C_2}\right) x \tag{8}$$

and finally the solution can be written as,

$$x^* = \mathbf{M_c}^{-1}{}_{C_1 C_2} \left(\mathbf{M}^T t_R\big|_{C_1} + \mathbf{M}^T t_R\big|_{C_2}\right) \tag{9}$$

where we obtain the solution for two load cases using

$$\mathbf{M_c}_{C_1 C_2} = \mathbf{M}^T \mathbf{M}\big|_{C_1} + \mathbf{M}^T \mathbf{M}\big|_{C_2} \tag{10}$$

This equation can be easily generalized to any number of load cases. Following the same reasoning, the variation on the parameters can be written as

$$x^* = \mathbf{M_c}^{-1} \sum_{k=1}^{N_C} \left(\mathbf{M}^T t_R\right)\big|_{C_k} \tag{11}$$

where $\mathbf{M_c} = \sum_{k=1}^{N_C} \left(\mathbf{M}^T \mathbf{M}\right)\big|_{C_k}$ and N_C is the number of load cases.

3. PHI Optics Unit

The method described has been applied for correlating the RTMM of Solar Orbiter PHI Optics Unit with its DTMM. The section 3.1 includes a brief description of the Solar Orbiter mission and the PHI instrument. Both the DTMM and the DTMM are described in section 3.2, followed with the results.
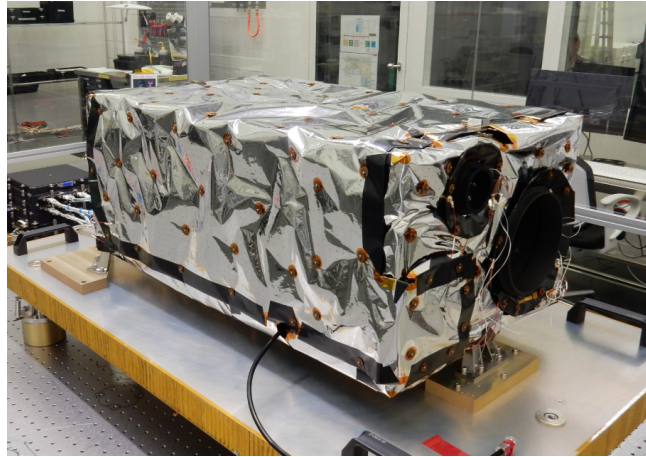

Figure 1: PHI O-Unit FM

3.1 Description of the PHI O-Unit

Solar Orbiter is a European Space Agency (ESA) mission whose main scientific objective is to understand how the Sun creates and modifies the heliosphere. It is a size-M mission scheduled to be launched in February of 2020 with an Atlas V Rocket from Cape Canaveral. It will reach a solar latitude of 34° with the perihelion of the orbit at 0.28 AU. During the perihelion, Solar Orbiter will receive a solar load equivalent to 13 solar constants. This makes the thermal design of the instruments onboard a difficult task.

PHI Optics Unit, with a size of 800 mm x 400 mm x 300 mm, consists of two structural blocks, made of the aluminium-beryllium alloy AlBeMet 162, joined to each other by six CFRP struts and a honeycomb panel. Attached to each aluminium block, one can find the different optical subsystems, their mechanisms, and the associated proximity electronics. The subsystems of this unit are: Primary Mirror (M1), Secondary Mirror (M2), Optics Baffle (OB), Common Power Converter (CPC), Correlation Tracker (CT), HRT Polarization Modulation Package (HPMP), HRT Re-Focus Mechanism (HRM), M4 assembly (M4), Full Disk Telescope (FDT), Feed Select Mechanism (FSM), Filtergraph (FG), and Focal Plane ssembly (FPA). In addition to this unit, two filters systems, the Heat Rejecting Entrance Windows (HREW), located in the entrance feed-through are also part of the instrument. Their purpose is to reject to space the solar radiation which is not of interest for PHI science, that is, they allow only a narrow band of electromagnetic radiation around 617.3 nm to enter the instrument. In addition to the subsystems, a connector panel (CP) is located on the Rear Block (RB), behind the Primary Mirror. All the elements within the optical cavity, with the exception of the optical elements (mirrors, lenses, etc.), are painted black to avoid straylight problems.

The unit is wrapped in 12-layer MLI to minimize the thermal radiation to the S/C. For cleanliness reasons the internal layers are VDA embossed perforated kapton. The inner surface is black kapton to avoid straylight within the unit and the outer layer is VDA-kapton, highly reflective to decouple the unit from the spacecraft. The MLI is held by means of an auxiliary support structure and is attached to the telescopes apertures by means of two Al7075 aluminum alloy rings. A photograph of PHI Optics Unit FM is shown in Figure 1.

3.2 Thermal and Geometrical Mathematical Model

The TMM consists of a system of differential equations that in the case of a steady-state analysis can be written as a system of ordinary equations as[7–9,12]

$$0 = Q_i + \sum_{j=1}^{n} GL_{ij}\left(T_j - T_i\right) + \sum_{j=1}^{n} GR_{ij}\sigma\left(T_j^4 - T_i^4\right) \tag{12}$$

where we have used the nomenclature from ESATAN-TMS, which is the software used and recommended by ESA for the Solar Orbiter mission. The *GL*s are the linear conductors, the *GR*s are the radiative conductors, σ is the Stefan-Boltzman constant and Q_i represents al the thermal loads in the node i.

The DTMM of PHI O-Unit consist of 7497 nodes. The model have been used to study the operational cases and the non-operational cases using steady-state and transient analyses. For this correlation two stady-state have been selected, the extreme hot and cold operational cases, here called C1 and C2 respectively.
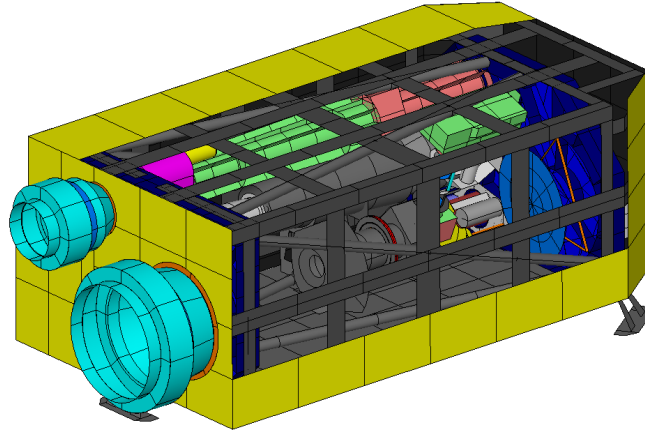

Figure 2: PHI O-Unit DTGMM

From the DTMM shown in Figure 2 a RTMM was derived. The reduction process[4] was done manually with the aim to keep physical meaning of all the parts. The maximum number of nodes for is model is 43 (35 + 8 boundary nodes) and this makes the reduction process a hard task. Many linear conductors have to merged and the estimated temperatures were outside the allowable margins. The figure 3 shows de RGMM with part of teh MLI removed so the subsystems can be seen. All the thermal nodes with representation in the DTMM have been condensed and are present in the RTMM as the model reduction has been carried out preserving the performance of the DTMM and always keeping the physical meaning of all the shells and thermal conductors.
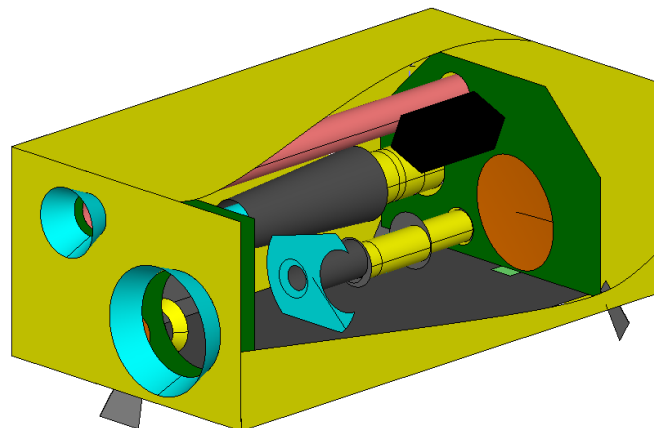

Figure 3: PHI O-Unit RTGMM

The linear conductors of RTMM are treated as parameters for the correlations process. This gives a total of 53 initial parameters to adjust. The Figure 4 shows the linears conductors, *GL*s present in the PHI O-Unit RTMM. It can be seen from the figure that all the subsystems are mounted in the FB or the RB but are quite isolate from each other. Therefore the parameters are expected to have a local effect on the temperatures.

To study the effect of each parameter in the temperatures of the model, the Figure 5 shows the influence, in variations of temperature of the nodes of the model against each parameter, *GL*s in this case. We can conclude that only 39 from the initial 53 parameters have a measurable influence in the model. Table 1 have the initial temperatures of the nodes estimated with the initial set of parameters. The discrepancy between the reference and the calculated
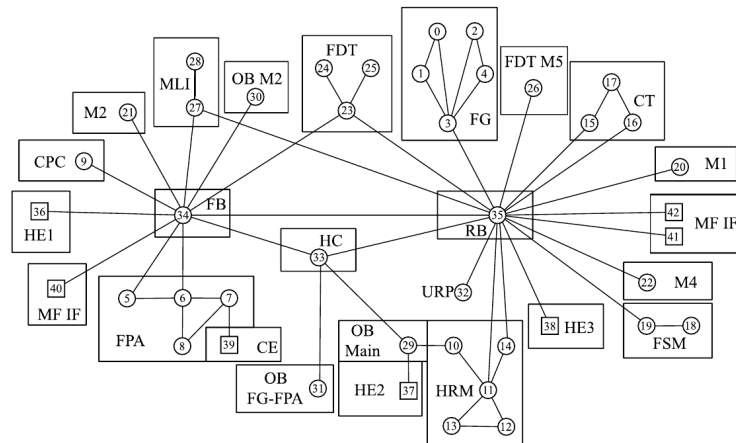
Figure 4: PHI O-Unit RTGMM Linear Conductors

temperatures is up to 51 °C in certain nodes. This model is far from being correlated.
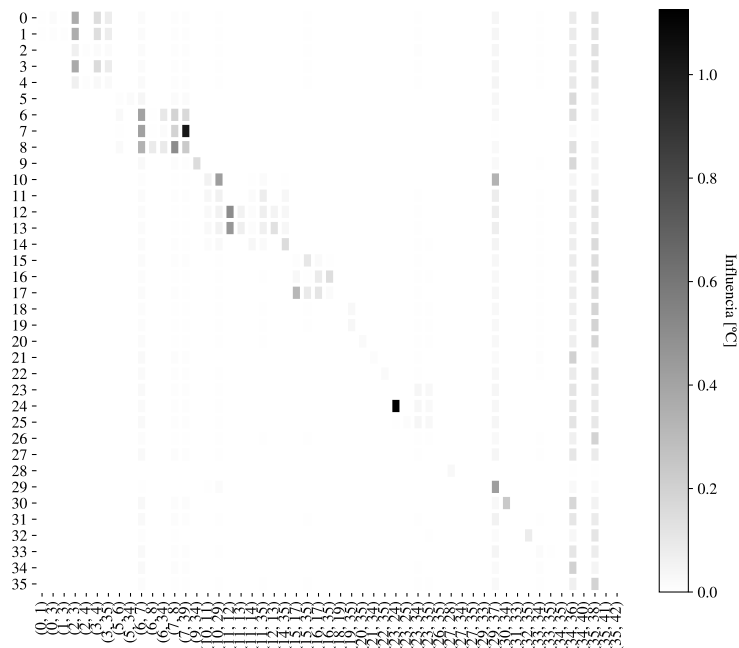
Figure 5: PHI O-Unit Influence of the parameters

3.3 Correlation criteria

Before correlating the model we have to define the criteria that we will use to consider a TMM correlated. This criteria is not clearly specified in the literature and may vary depending on the project. We will consider a good correlation based in the ECSS recommendations.[2] These recommendations are given for the correlation against test data, but as the goal hete is very similar it can be extended to the correlations of the RTMMs. The deviations between the two models must be kept as follows:

- Maximum temperature difference between DTMM and RTMM < 3K for internal equipment and < 20K for MLIs.

Table 1: PHI OPT. RTMM Initial temperatures

		Reference Temperature °C		Initial Temperature °C		ΔT °C	
Node	Label	C1	C2	C1	C2	C1	C2
0	FG Etalon	65.9	66.5	66.21	17.04	-0.3	49.5
1	FG Pre Filter	65.2	63.3	66.14	16.77	-0.9	46.5
2	FG Struct Ext	57.0	14.2	65.72	14.68	-8.7	-0.5
3	FG Struct Int	65.9	65.7	66.26	17.22	-0.4	48.5
4	FG Lenses	57.4	17.5	63.99	5.67	-6.6	11.8
5	FPA Baffle	51.5	-18.3	59.91	-16.75	-8.4	-1.5
6	FPA Sturcture	46.8	-16.9	45.92	-16.30	0.9	-0.6
7	FPA APS	2.1	-20.7	1.29	-21.29	0.8	0.6
8	FPA PCB	53.3	-9.5	34.56	-6.08	18.7	-3.4
9	CPC CPC	53.6	-16.4	64.79	-9.10	-11.2	-7.3
10	HRM FS0	59.7	-17.6	77.53	-8.32	-17.8	-9.3
11	HRM Structure	56.4	-11.5	70.19	-6.79	-13.8	-4.7
12	HRM LCVR	75.0	45.2	71.74	0.45	3.3	44.7
13	HRM Polarizer	78.5	46.5	71.08	-4.75	7.4	51.2
14	HRM FS1	54.8	-14.5	69.78	-7.49	-15.0	-7.0
15	CT Structire	54.1	-16.3	62.34	-14.40	-8.2	-1.9
16	CT Detector	55.6	-14.7	68.87	-5.61	-13.3	-9.1
17	CT PCB	64.2	-4.6	69.92	-4.26	-5.7	-0.3
18	FSM M3	52.4	-17.2	63.11	-13.37	-10.7	-3.8
19	FSM FS2	54.0	-15.3	63.18	-13.32	-9.2	-2.0
20	M1 M1	52.0	-18.7	62.20	-14.89	-10.2	-3.8
21	M2 M2	51.1	-19.8	59.97	-16.97	-8.9	-2.8
22	M4 M4	52.7	-13.6	61.66	-14.23	-9.0	0.6
23	FDT Structure Tube	54.9	-17.6	61.72	-15.63	-6.8	-2.0
24	FDT LCVR	74.8	-5.4	67.02	-13.71	7.8	8.3
25	FDT Lenses	54.2	-18.0	61.83	-15.61	-7.6	-2.4
26	FDT M5	51.9	-18.5	61.73	-14.79	-9.8	-3.7
27	MLI Internal Layer	52.9	-18.5	61.16	-16.40	-8.3	-2.1
28	MLI External Layer	50.3	-19.9	60.63	-16.48	-10.3	-3.4
29	OB Main	54.4	-19.0	75.74	-12.78	-21.3	-6.2
30	OB M2	58.4	-19.5	66.34	-16.95	-7.9	-2.5
31	OB FPA-FG	53.7	-16.3	62.08	-15.06	-8.4	-1.2
32	URP URP	50.7	-19.5	60.50	-15.33	-9.8	-4.2
33	HC HC	52.5	-18.8	61.15	-16.32	-8.6	-2.5
34	FB FB	51.6	-19.7	59.80	-16.98	-8.2	-2.7
35	RB RB	51.6	-18.7	61.73	-14.78	-10.1	-3.9

- Difference in the heat flux across spacecraft interfaces < 10 % when the heat flux is grater than 1 W and 0.1 W when is less.

- Difference in the consumed heater power < 10 %.

3.4 Results

The method proposed have been applied and after 13 iterations the method converged to a set of parameters used to estimate the temperatures given in the Table 2.

- In the load case C1, the maximum difference in the nodes temperature have decreased from 21.3 °C to 2.9 °C. All the nodes are within the margins.

- In the load case C2, the maximum difference in the nodes temperature have decreased from 51.2 °C to 2.6 °C. All the nodes are within the margins.

The next step is to calculate the heat flux through the interfaces. The fluxes for the case C1, which correspond to the hot operational case is shown in Table 3. In the table is also presented the reference values and the initial estimation of the heat fluxes. The initial estimation have been made using the the initial values of the parameters. In brackets, the difference between the estimated value and the reference value is shown. Not all values are within the allowable range, the heat flux though the feet and the radiative spacecraft cavity are out of limits by 0.6 W. This discrepancy is quite low compared to the total heat power that is 22 W.

Table 2: PHI OPT. Final temperatures

Node	Label	Reference Temperature °C		Final Temperature °C		ΔT °C	
		C1	C2	C1	C2	C1	C2
0	FG Etalon	65.9	66.5	68.03	66.26	2.13	0.24
1	FG Pre Filter	65.2	63.3	67.81	65.29	2.61	1.99
2	FG Struct Ext	57.0	14.2	58.01	12.84	1.01	1.36
3	FG Struct Int	65.9	65.7	68.47	68.19	2.57	2.49
4	FG Lenses	57.4	17.5	58.69	15.79	1.29	1.71
5	FPA Baffle	51.5	-18.3	53.57	-18.70	2.07	0.40
6	FPA Sturcture	46.8	-16.9	49.19	-14.97	2.39	1.93
7	FPA APS	2.1	-20.7	3.09	-20.89	0.99	0.19
8	FPA PCB	53.3	-9.5	50.62	-9.70	2.68	0.20
9	CPC CPC	53.6	-16.4	56.16	-15.55	2.56	0.85
10	HRM FS0	59.7	-17.6	61.75	-16.90	2.05	0.70
11	HRM Structure	56.4	-11.5	58.62	-11.79	2.22	0.29
12	HRM LCVR	75.0	45.2	76.02	46.36	1.02	1.16
13	HRM Polarizer	78.5	46.5	78.25	45.02	0.25	1.48
14	HRM FS1	54.8	-14.5	56.73	-15.21	1.93	0.71
15	CT Structire	54.1	-16.3	56.95	-14.04	2.85	2.26
16	CT Detector	55.6	-14.7	55.75	-15.57	0.15	0.87
17	CT PCB	64.2	-4.6	65.41	-2.93	1.21	1.67
18	FSM M3	52.4	-17.2	54.33	-17.37	1.93	0.17
19	FSM FS2	54.0	-15.3	54.32	-17.36	0.32	2.06
20	M1 M1	52.0	-18.7	54.33	-17.74	2.33	0.96
21	M2 M2	51.1	-19.8	53.55	-19.03	2.45	0.77
22	M4 M4	52.7	-13.6	54.63	-16.02	1.93	2.42
23	FDT Structure Tube	54.9	-17.6	55.62	-17.81	0.72	0.21
24	FDT LCVR	74.8	-5.4	77.53	-8.01	2.73	2.61
25	FDT Lenses	54.2	-18.0	55.82	-17.78	1.62	0.22
26	FDT M5	51.9	-18.5	53.85	-17.79	1.95	0.71
27	MLI Internal Layer	52.9	-18.5	54.71	-18.39	1.81	0.11
28	MLI External Layer	50.3	-19.9	50.32	-19.79	0.02	0.11
29	OB Main	54.4	-19.0	55.96	-19.13	1.56	0.13
30	OB M2	58.4	-19.5	57.32	-19.03	1.08	0.47
31	OB FPA-FG	53.7	-16.3	55.03	-16.83	1.33	0.53
32	URP URP	50.7	-19.5	52.30	-18.67	1.60	0.83
33	HC HC	52.5	-18.8	54.71	-18.39	2.21	0.41
34	FB FB	51.6	-19.7	53.14	-19.07	1.54	0.63
35	RB RB	51.6	-18.7	53.83	-17.79	2.23	0.91

4. Conclusion

A new method for the correlation of thermal mathematical models with reference data have been presented. The method, based on Jacobian matrix formulation (Taylor series expansion) and solved using the Moore-Penrose pseudo-inverse matrix, has been applied to the correlation of the PHI O-Unit RTMM of the Solar Orbiter ESA mission.

The correlation of the thermal mathematical model to a reference temperature data is a task that any thermal engineer must confront sooner or later in the common development path of a space project. The results of the models

Table 3: Heat flux through the spacecraft interfaces. Load case C1

Interface	Reference value	Initial estimation		Final estimation	
HE IF 1	6.8 W	9.9 W	(46%)	7.0 W	(3%)
HE IF 2	7.1 W	3.6 W	(-49%)	6.7 W	(-6%)
HE IF 3	4.7 W	3.3 W	(-30%)	4.7 W	(0%)
CE IF	3.1 W	5.1 W	(65%)	3.1 W	(0%)
Feet	0.1 W	0.1 W	(0.0 W)	0.5 W	(0.4 W)
S/C (Radiative)	0.2 W	<0.05 W	(0.2 W)	<0.01 W	(0.2 W)

have to be in agreement with the temperatures measured in the TVAC tests or the flight data. The RTMM must (or intend to) predict the same temperatures that the corresponding DTMM. In any case the correlation must be carried out and the source of the reference data is not important.

This correlation is usually done manually and requires an enormous effort in terms of time and therefore, cost. The intention of the method proposed is to provide the thermal engineer with the tools required to incorporate the model correlation to the normal workflow of the thermal design.

The method have been applied to the PHI O-Unit RTMM. The intention was to demonstrate that the correlation method can be applied to a larger model but small enough to be able to be understandable by a person from outside the project. The model has 35 temperatures points to be correlated with the results from two load cases. This model has been presented and its parameters analyzed. A total of 39 parameters were selected for the correlation and the results provided by the correlated model shows that the temperatures obtained are inside the common requirements used in space programs.

5. Acknowledgments

References

[1] T. Akita, R. Takaki, and E. Shima. A new adaptive estimation method of spacecraft thermal mathematical model with an ensemble Kalman filter. *Acta Astronautica*, 73:144–155, 2012.

[2] ESA Requirements and Standards Division. ECSS-E-ST-31C - Space Engineering, Thermal control general requirements, 2008.

[3] European Space Agency. Solar orbiter. [Online; accessed <today>].

[4] Germán Fernández-Rico. *Quasi-Autonomous Spacecraft Thermal Model Reduction*. PhD thesis, Universidad Politécnica de Madrid Escuela, Escuela Técnica Superior de Ingeniería Aeronáutica y del Espacio Doctoral, 2018.

[5] B (Airbus Safran Launchers Gmbh) Frey, M (Airbus Defence Trinoga, Space GmbH), M Hoppe, W (Airbus Defence Ebeling, and Space GmbH). Development of an Automated Thermal Model Correlation Method and Tool. In *44th International Conference on Environmental Systems (ICES)*, 2015.

[6] Iñaki Garmendia and Eva Anglada. Thermal mathematical model correlation through genetic algorithms of an experiment conducted on board the International Space Station. *Acta Astronautica*, 122:63–75, 2016.

[7] David G Gilmore. *Spacecraft Thermal Control Handbook. Volume I*, volume I. El Segundo, California, Aerospace Press, 2002.

[8] ITP Engines UK Ltd. Esatan-tms thermal engineering manual. Technical report, ITP Engines UK Ltd. Whetstone, Leicester, UK, 2015.

[9] Robert Karam. *Satellite Thermal Control for Systems Engineers*. American Institute of Aeronautics and Astronautics, Inc, 2012.

[10] Jan Klement, Eva Anglada, and Iñaki Garmendia. Advances in automatic thermal model to test correlation in space industry. *46th International Conference on Environmental Systems*, pages 1–11, 2016.

[11] Donald W Marquard. An Algorithm For Least-Squares Estimation Of Nonlinear Parameters. *Journal of the Society for Industrial and Applied Mathematics*, 11(2):431–441, 1963.

[12] Jose Meseguer, Isabel Pérez-Grande, and Angel Sanz-Andrés. *Spacecraft Thermal Control*. Woodhead Publishing, 2012.

[13] Ignacio Torralbo, Isabel Perez-Grande, Angel Sanz-Andres, and Javier Piqueras. Correlation of spacecraft thermal mathematical models to reference data. *Acta Astronautica*, 144(November 2017):305–319, 2018.